Article

Not peer-reviewed version

Hair-Reinforced Elastomer Matrix Composites: Formulation, Mechanical Testing and Advanced Microstructural Characterization

Eugene S. Statnik *, Julijana Cvjetinovic, Semen D. Ignatyev, Loujain Wassouf, Alexey I. Salimon, Alexander M. Korsunsky

Posted Date: 4 October 2023

doi: 10.20944/preprints202310.0222.v1

Keywords: hair; polymer; composite; carbon; fracture; SEM

Article

Hair-Reinforced Elastomer Matrix Composites: Formulation, Mechanical Testing and Advanced Microstructural Characterization

Eugene S. Statnik [1], Julijana Cvjetinovic [2], Semen D. Ignatyev [1], Loujain Wassouf [3], Alexey I. Salimon [1] and Alexander M. Korsunsky *

[1] <<LUCh>> lab, NUST MISIS, Moscow, Russia
[2] Center for Photonic Science and Engineering, Skoltech, Moscow, Russia
[3] Department of Physical Chemistry, NUST MISIS, Moscow, Russia
* Independent researcher (Principle investigator); *alexander.korsunsky@gmail.com*

Abstract: Epoxy matrix composites reinforced with high-performance fibers such as carbon, Kevlar, and glass, exhibit excellent specific stiffness and strength in many mechanical applications. However, these composites are disappointingly non-recyclable and are usually disposed of in landfill sites, with no realistic prospect for biodegradation in reasonable time. In contrast, moldable composites with carbonized elastomeric matrices developed in the last decades possess attractive mechanical properties in final net-shape products and can also be incinerated or recycled. Many carbon and inorganic fillers have recently been evaluated to adjust the properties of carbonized elastomeric composites. Renewable organic fillers such as human or animal hair offer an attractive fibrous material with substantial potential for reinforcing composites with elastomeric matrices. Samples of unidirectional fiber composites (with hair volume fraction up to 7 %) and quasi-isotropic short fiber composites (with hair volume fraction up to 20 %) of human hair-reinforced nitrile butadiene rubbers (HH-NBR) were produced in the peroxide-cured and carbonized states. The samples were characterized using SEM, Raman spectroscopy and photoacoustic microscopy. Mechanical tests were performed in tension using a miniature universal testing machine. The expected effect of fiber reinforcement on the overall mechanical performance has been demonstrated for both cured and carbonized composites. Considerable enhancement of the elastic modulus (up to 10 times), ultimate tensile strength (up to 3 times) and damage tolerance was achieved. The evidence of satisfactory interfacial bonding between hair and rubber was confirmed by SEM imaging of fracture surfaces. The suitability of photoacoustic microscopy was assessed for 3D reconstruction of the fiber sub-system spatial distribution and non-destructive testing.

Keywords: hair; polymer; composite; carbon; fracture; SEM

1. Introduction

Hair is a readily available, affordable, renewable and durable biopolymer material that is well known and traditionally applied by humans for fabrication and construction since the Neolithic epoch [1]. Human hairs and animal bristles have been used for diverse house appliances (e.g., brushes and polishing tools), construction materials, bijouterie, clothing, musical instruments, and, more specifically, in mechanical applications to reinforce technical fabrics and insulating mats [2], clay [3], brick and concrete [4].

Recently, human hairs have been evaluated as reinforcing fibers in epoxy composites [5] and 3D-printable PLA [6]. Taking into account that hairs do not exhibit outstanding specific stiffness and strength when compared to many other fibrous materials as shown in Figure 1, it is necessary to provide strong arguments to justify their use for polymer matrix reinforcement in engineering composites.

Preprints (www.preprints.org) | NOT PEER-REVIEWED | Posted: 4 October 2023 doi:10.20944/preprints202310.0222.v1

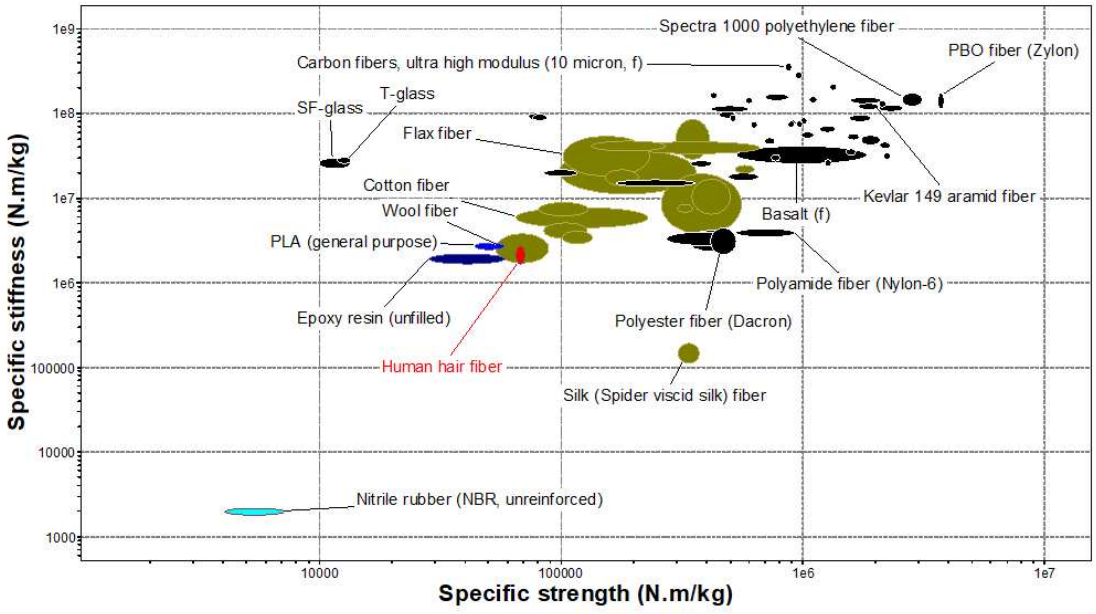

Figure 1. Ashby's chart for mechanical performance of fiber materials.

We formulate such arguments as follows:

- *Eco-friendliness*. Since the hairs are bioderived fibers based on the natural polymer keratin, they represent a natural, cheap, renewable, and biodegradable alternative to polyester, glass and carbon fibers. However, it should also be noted that cellulose-based fibers derived from plants such as flax and cotton can be readily produced at an industrial scale and generally have superior reproducibility of mechanical properties.
- *Attractive surface structure*. Hair is a complex, hierarchically structured object with intricate internal and surface [7] structure, which has been extensively studied using various microscopy and tomography methods over decades [8]. Keratin scales on the surface of hair fibers are considered to be effective mechanical hooks for providing a strong interface bond with the matrix, which can be further improved through chemical modification (activation).
- *Rational choice of matrix material*. Hairs are very flexible in bending and in tension show large values of elongation to rupture of up to 50 %. The specific strength and stiffness of hairs are almost identical to epoxy and PLA, indicating that little or no reinforcement effect can be anticipated in composites using these matrices. The overall mechanical performance of hairs (low stiffness and good flexibility) suggests that the reinforcement effect is likely to be more pronounced for polymer matrices with lower stiffness, such as elastomers.

In this article, we examine some aspects of hair fiber reinforcement for elastomer matrix composites. To the best of our knowledge, it is the first report on human hair-nitrile butadiene rubber (HH-NBR) composites that have been intentionally formulated, fabricated, characterized, and tested to investigate the potential of this class of engineering materials.

NB rubber compounds have various applications in the oil and gas, chemical, automotive and general engineering industries due to their excellent combination of mechanical performance, chemical stability, water and solvent resistance, as well as temperature resistance. Various inorganic fillers, such as carbon black, graphite, silica, etc. along with curing and processing agents, are added to the NB *caoutchouc* by industrial producers to tailor the properties of the vulcanized compound and to match the requirements posed by the specific service conditions.

In the last decade, a specific class of carbon-based composites known as carbonized elastomeric composites have been developed [9]. These composites aim to combine the benefits of traditional rubber technology, such as high filling ratio and precise molding, with gentle low-temperature carbonization, ultimately targeting the mass-production of high-quality engineering parts with high mechanical performance [10]. This class of materials is a competitor of magnesium and aluminum

 doi:10.20944/preprints202310.0222.v1

alloys in terms of mechanical performance, but offers advantages in chemical and temperature resistance [11].

We fabricated unidirectional and quasi-isotropic short fiber composites by introducing human hair reinforcements (without any other fillers) into a peroxide curable NB *caoutchouc* (natural isoprene) matrix. Plates of composites were thermally pressed to vulcanize the NB matrix and to prepare elastomers for subsequent carbonization. The vulcanized and carbonized composites were characterized using SEM, Raman spectroscopy and photoacoustic microscopy. The latter technique utilizes photoacoustic effect of melanin present in hairs as natural pigment. This has been applied for the first time in composite material science to obtain non-destructive visualization of the internal filler spatial distribution in 3D. We discuss the appearance of fracture surfaces in samples after tensile mechanical testing in connection with strong reinforcement effect caused by hairs both in vulcanized and carbonized composites.

2. Materials and methods

2.1. Samples preparations

The nitrile-butadiene caoutchouc BNKS-18 (Sibur Inc., Krasnoyarsk, Russia) was cut into pieces for softening and repeatedly rolled for 10 min using laboratory two roll rubber mill BL-6175-A (Dongguan Baopin Precision Instrument Co., Dongguan, China) to intermix caoutchouc with human hairs and dicumyl-peroxide ($C_{18}H_{22}O_2$, CAS number 80-43-3, Sigma-Aldrich Corp., St. Louis, MO, USA). "Pristine" human hairs of average length of about 100 mm were donated in their natural state by one of authors to the total amount of 185 g. The human hair has not been previously undergone any chemical, thermal, or coloring treatments.

To produce unidirectional composites, a significant amount (up to 400 g) of rubber was rolled to a thickness of 1.5 mm. Long human hairs (approximately 8 g per 100 g of NB cauthchouque) were introduced into the inter-roll gap manually guiding the hairs to run parallel to the rolling direction. The compound was mixed for 25 min at a temperature of approximately 80 °C. Then, the mixture was cooled down to 40 °C before introducing 3 g of the dicumyl-peroxide per 100 g of NB caoutchouc to produce rubber compound. The duration of the final mixing stage was 10 min to ultimately obtain 1.2~1.4 mm thick sheet of compound ready for vulcanization. This sheet was cut into 145×145 mm^2 squares. Next, they were put in stacks of 6 slices, which allowed to create the 0/0/0/0/0/0 and 0/90/0/90/0/90 stacking sequences. Stacks were vulcanized under plate compression to 10 MPa pressure at 170 °C for 10 min in air using an automated hydraulic 40 tons press (Tesar Engineering Ltd., Saratov, Russia). Vulcanized sheets having thickness of about 3.5 mm were cut using a hardened steel punching tool to obtain dog-bone samples for tensile testing. Varying the orientation of the punching tool, specimens with hair reinforcements oriented parallel (II) or perpendicular (=) to gage axis were produced from 0/0/0/0/0/0 stacks. Additionally, specimens with hair reinforcements oriented both parallel and perpendicular were cut from 0/90/0/90/0/90 stacks after vulcanization. Due to the limited amount of long hairs from a particular person, only a few samples with the specified dimensions could be produced and therefore statistical analysis is limited too. Unfortunately, the attempts to increase the filling ratio for unidirectional composites also failed using the current technology because long hairs tended to break into shorter pieces during mixing and lose their desired orientation.

Quasi-isotropic composites were fabricated similarly, i.e. long hairs were cut onto segments chopped down to 20 mm and randomly introduced into NB caoutchouc matrix, which was then freely poured onto the surface of another caoutchouc material entrapped between mill rolls. In contrast to unidirectional composites, the volume fraction of reinforcing fibers in the former could be increased up to 20 % to investigate the impact of a high filling ratio. Moreover, the use of miniature specimens for in-SEM mechanical testing allowed improving statistics and increasing fidelity.

2.2. Scanning electron microscopy

Preprints (www.preprints.org) | NOT PEER-REVIEWED | Posted: 4 October 2023 doi:10.20944/preprints202310.0222.v1

The fracture surfaces of both vulcanized and carbonized types of samples as well as hairs distribution and structure were investigated by a versatile FIB-SEM Tescan Amber (TESCAN GROUP, Brno, Czech Republic) under the following conditions: SE detector, working distance of 6 mm, landing energy of 5 kV, beam current of 300 pA, 2K image size with 8-bit depth. Prior to investigation the samples were sputtered with a very thin layer of gold nanoparticles using Quorum Q150R ES Magnetron machine (Quorum Technologies, Judges Scientific, Lewes, UK).

2.3. Tensile test

Mechanical tests of the produced samples were conducted using a Zwick/Roell Z020 (Zwick GmbH, Ulm, Germany) universal testing machine equipped with a MultiXtens high-precision strain measuring system for large samples and a Deben MT 1 kN tensile tester (Deben UK Ltd., Woolpit, UK) for miniature samples, respectively. The sketches of the typical size and shape of the specimens are presented in Figure 2.

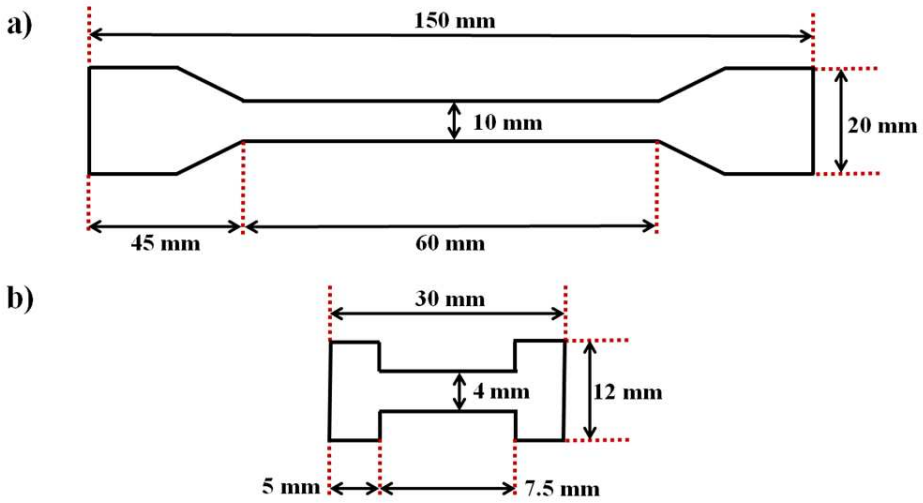

Figure 2. The sketch of the a) large and b) miniature samples.

The large specimens were tested at a constant crosshead speed of 2 mm/min, while the miniature ones were examined at a half that rate. The tests were carried out in an open-air environment and recorded using a digital camera. Subsequently, the resulting videos were processed with the free trial version of the commercial GOM Correlate Pro Digital Image Correlation (DIC) software (Carl Zeiss GOM Metrology GmbH, Braunschweig, Germany) to determine the true strains within the samples.

The number of samples with different filling ratio and orientation was limited to 2 due to technological constraints. The proposed method made it challenging to align and reinforce larger samples. In contrast, 5 miniature specimens were employed to examine data dispersion. In this case, to localize deformation at the center of the specimen, small incisions were made on both sides perpendicular to the axis of tension with a depth of 0.5 mm and a width of 0.2 mm. The various miniature sample prepared by this method are shown in Figure 3.

Preprints (www.preprints.org) | NOT PEER-REVIEWED | Posted: 4 October 2023 doi:10.20944/preprints202310.0222.v1

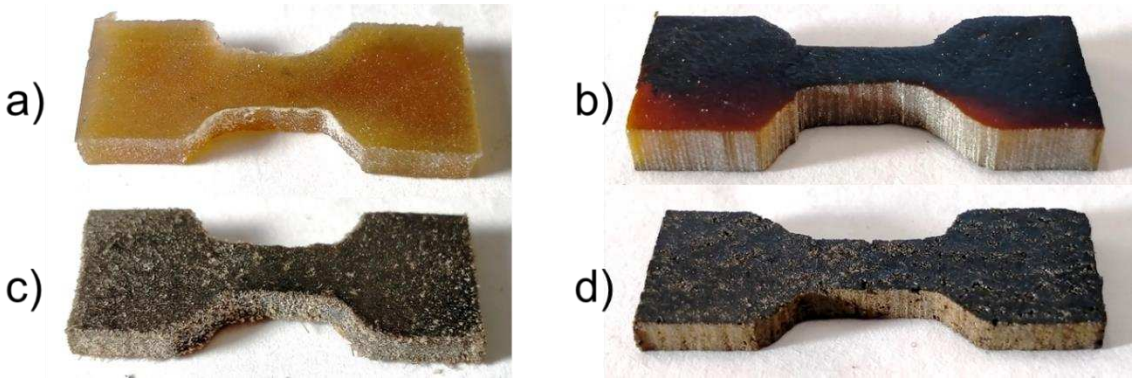

Figure 3. The appearance of the prepared miniature samples: a) before carbonization **without** hairs, b) after carbonization **without** hairs, c) before carbonization **with** hairs, d) after carbonization **with** hairs.

2.4. Photoacoustic microscopy

The Raster Scanning Optoacoustic Mesoscopy system RSOM Explorer P50 (iTheraMedical GmbH, Munich, Germany) was employed to acquire photoacoustic signals from hair-reinforced elastomer matrix composites as well as raw elastomer matrix. Prior to imaging, the samples were placed in a plastic container and submerged in deionized water to ensure adequate ultrasound coupling with the transducer. Optical excitation was achieved using a Wedge-HB frequency-doubled flashlamp-pumped Nd:YAG laser (1064/532 nm wavelength, 1 ns pulse duration, 200 μJ pulse energy, 1 kHz repetition rate) delivered through a 2-arm glass fiber bundle, resulting in a spot size ranging from 3.5 to 5.0 mm [12,13]. The scanning was performed in the field of view up to 12×12 mm^2 with depths of up to 3 mm and a step size of 20 μm. To detect the induced ultrasound signals, a custom-made spherically focused $LiNbO_3$ detector with parameters including a center frequency of 50 MHz, bandwidth of 11-99 MHz, focal diameter of 3 mm, and focal distance of 3 mm was utilized. The RSOM setup provided axial and lateral resolution capabilities of 10 μm and 40 μm, respectively. The resulting signals were displayed in frequency ranges of 11-33 MHz (shown in red) and 11-99 MHz (merged).

3. Results and discussion

3.1. Microstructure characterization by scanning electron microscopy

SEM images of a BN rubber-based vulcanized composite with a 7 vol. % hair reinforcement (in a mixed orientation with respect to the tension axis) taken at different magnifications are shown in Figures 4 and 5. The fracture surface exhibits intricate relief with flat regions in the matrix, alongside many steps and well-preserved reinforcing hairs with characteristic 'scale-like' surface features. The presence of smooth facets and step features indicates the prevalence of the brittle failure mechanism. No micro–cracks are evident, but single tears are present as seen in Figure 4a).

To assess the adhesion between hairs and matrix in the composites, SEM images of the hair surface morphology and matrix channels were analyzed. Several images reveal the characteristic imprints of hair surface morphology on the matrix after removal (such as tearing or loss of cohesion), indicating satisfactory adhesion. This suggest the establishment of a strong mechanical bond between the human hair fibers and the matrix as illustrated in Figures 4b) and 4d).

The pattern of the hair-matrix interface and structure of the fractured hairs shown in Figures 5b) and 5c), respectively, indicate that hair breaks under tension in a brittle manner, resulting in a relatively flat area on the fracture zone across the entire cross-section of the hair and a precise imprint of the hair structure in the matrix. Another fracture mechanism was also observed, in which a portion of the matrix material tears out along with the hair undergoing plastic flow and ductile fracture due to sufficient hair-matrix adhesion. This mechanism can be found in Figure 5c).

Preprints (www.preprints.org) | NOT PEER-REVIEWED | Posted: 4 October 2023 doi:10.20944/preprints202310.0222.v1

The hair surface is not smooth but displays scale-like nature that improves the cohesion through mechanical 'keying in' within the matrix. The surface of human hair is naturally scaly. The small scales located at the hair surface create tiny steps or wedges. When the fibers are mixed with rubber, the rubber molecules penetrate these wedges, enhancing the physical interaction. This interaction between human hair and rubber improves the overall physical and mechanical properties. Some of the characteristics of human hair fibers that make them a promising reinforcement and strengthening material due to their excellent tensile strength, slow degradation rate, hydrophilic properties, affordability, distinctive chemical composition, and elastic recovery capability.

The fracture structure of carbonized composite with hair reinforcement based on BN rubber shown in Figure 6 differs from vulcanized one due to its increased smoothness, namely, with larger flat facets, lack of protruding free ends of reinforcing hairs from the matrix, and the formation of pores in empty channels following hair pull out.

The reinforcing fibers may have an inhomogeneous distribution throughout the matrix. The fracture of the fiber takes the shape of a smooth, concave rounded area with a set of cracks running parallel to the hair axis. This effect might be linked to thermal degradation. The cracks may propagate into the matrix, leading to the conclusion that carbonized hairs are no longer useful as effective crack blockers. The carbonization process results in a loss of the hair connectivity with the matrix, at least for a part of the reinforcing hair. Consequently, the hair-matrix interface is apparently weakened, making it easier for the reinforcing component to be pulled out from the matrix.

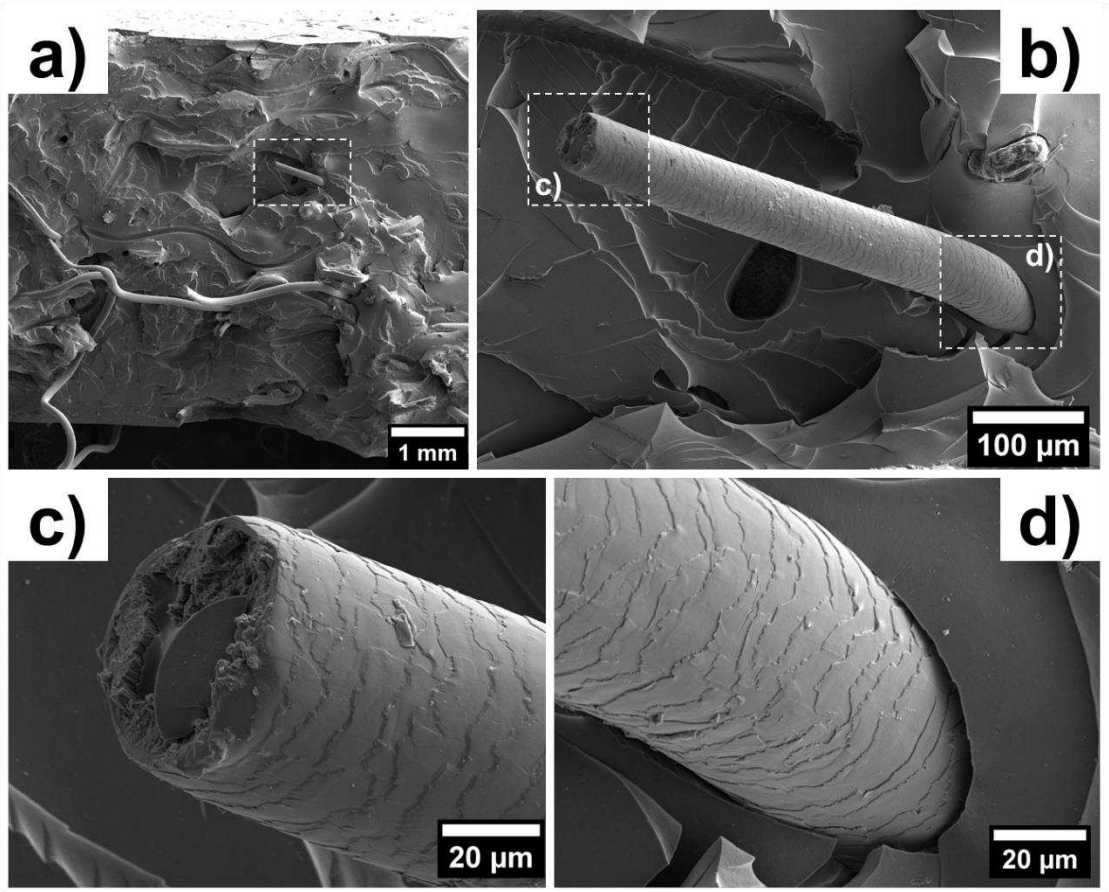

Figure 4. The fracture surface of a BN rubber-based vulcanized composite with a 7 vol. % hair reinforcement: a) general view with indication of specific protruding hair from polymer matrix as a white dashed rectangular, b) detailed view of the hair structure with two selected regions like c) fracture zone and d) the interface between hair and matrix.

Preprints (www.preprints.org) | NOT PEER-REVIEWED | Posted: 4 October 2023 doi:10.20944/preprints202310.0222.v1

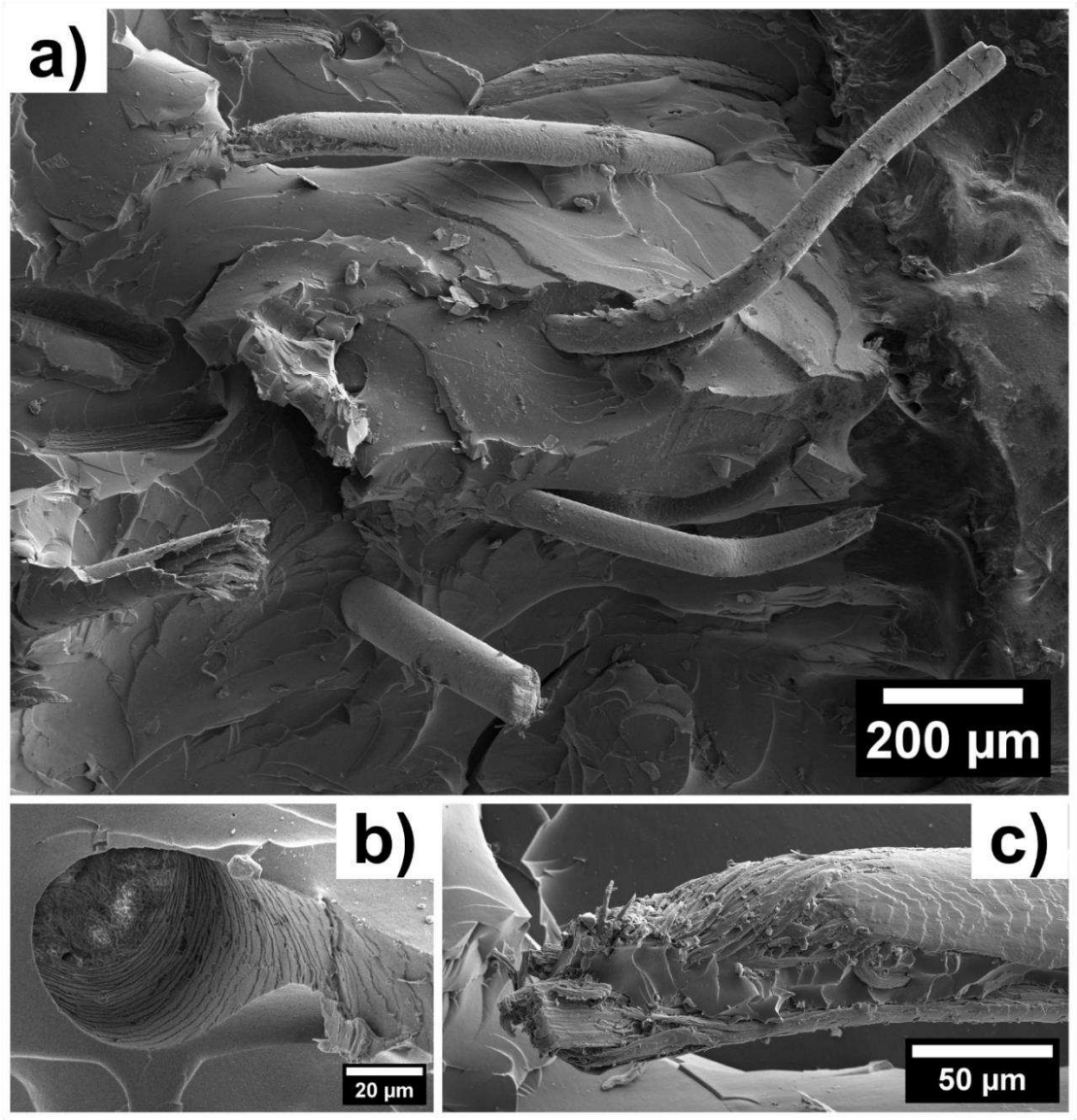

Figure 5. The counterpart of the fracture surface demonstrated in Figure 4: a) large overview, b) imprint of hair structure at the lacuna (matrix) periphery with the visible cross-section of fractured hair at the bottom [*first fracture mechanism*], c) appearance of hair structure after removal from polymer matrix [*second fracture mechanism*].

Preprints (www.preprints.org) | NOT PEER-REVIEWED | Posted: 4 October 2023 doi:10.20944/preprints202310.0222.v1

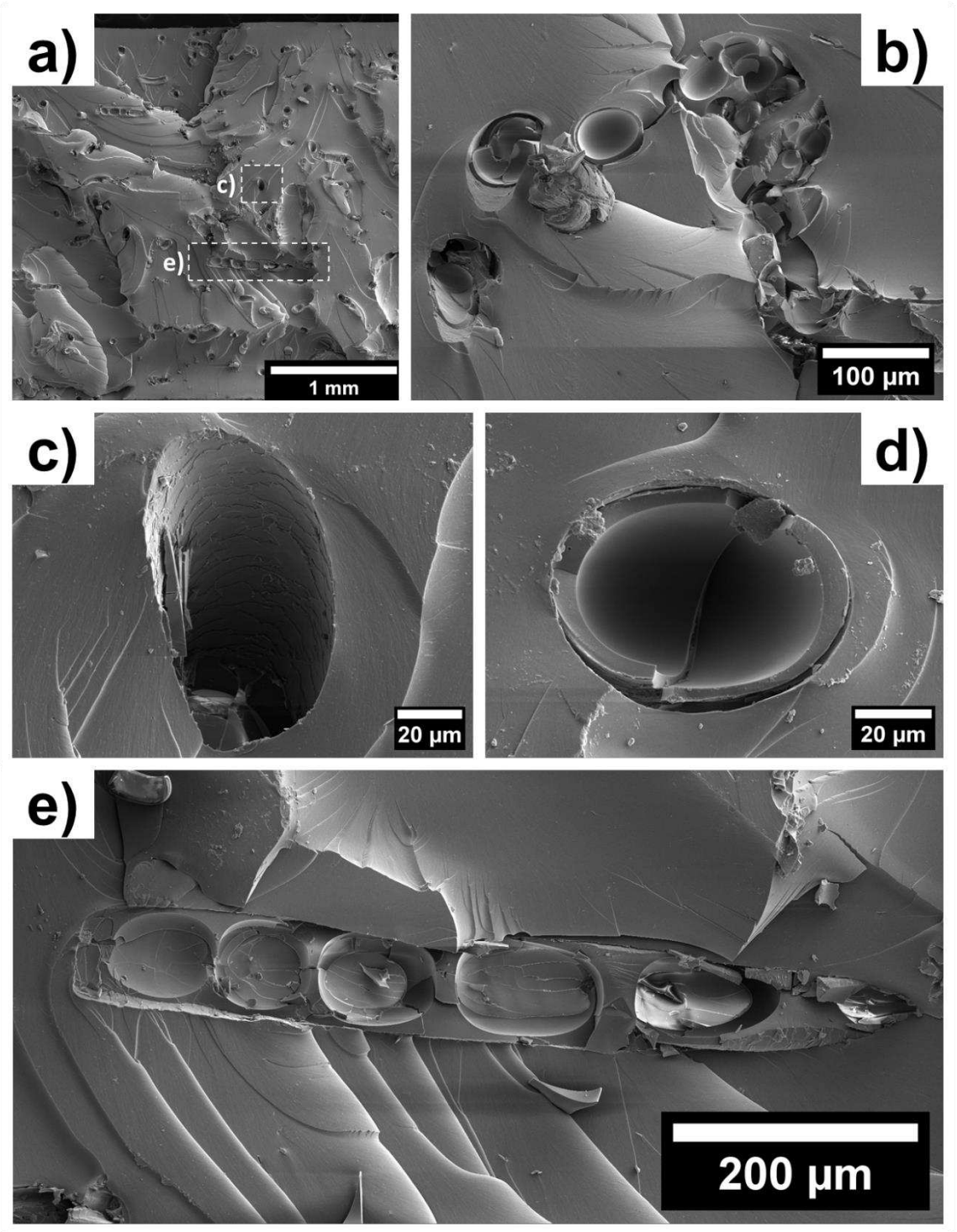

Figure 6. The fracture surface of a BN rubber-based carbonized composite with a 7 vol. % hair reinforcement: a) general view with the indication of b) cross-section of the hairs conglomerate accumulated in the matrix due to poor mixing, c) lacuna received after tension test, d) cross-sectional view of the hair structure, e) longitudinal slice of the fractured hair.

Based on the obtained views of the hair-composite microstructure, several approaches can be recommended to enhance the mechanical properties of vulcanized and carbonized elastomer composites reinforced with the addition of hair fibers, including

- the optimization of the carbonization temperature to prevent the hair biopolymer thermal destruction;

Preprints (www.preprints.org) | NOT PEER-REVIEWED | Posted: 4 October 2023 doi:10.20944/preprints202310.0222.v1

- the chemical modification of the hair surface to enhance its adhesion to the elastomeric matrix homogenizing the composite during rubber mixture preparation.

3.2. Mechanical properties measurements

The stress-strain curves obtained for large samples are shown in Figure 7. The correspondent mechanical characteristics were estimated and summarized in Table 1.

There is a distinct correlation between Young's modulus and the orientation of reinforcing hairs relative to the tension axis. Specifically, vulcanized samples with reinforcing hairs parallel to the tension axis have an elastic modulus that is 40 % higher than those with perpendicular or mixed orientation. This phenomenon aligns with the rule-of-mixtures corresponding to the Voigt and Reuss models. In contrast, the orientation of hairs does not impact the ultimate strength and elongation to rupture. The values are distributed within a narrow range from 1.0 to 1.2 MPa and from 15 to 23 %, respectively.

The ultimate strength of carbonized specimens reached a maximum of 7.8 MPa when the reinforcing hair fibers were parallel to the tension axis. At the same time, samples with mixed orientation of fibers had the lowest elongation to rupture with a value of 0.02 %. The elastic modulus of the carbonized composites do not show clear dependence on fiber orientation.

On the other hand, carbonization of the vulcanized specimens entailed noticeable increase in Young's modulus and ultimate strength in general. For instance, the elastic modulus increase varied from 200 to 350% (when the reinforcing hairs were oriented parallel to the tension axis), and from 400 to 500% (when the reinforcing hairs were oriented perpendicular to the tension axis) and increased by up to 250% (when the reinforcing hairs were placed in mixed manner), respectively. Moreover, the ultimate strength increase by a factor of 3.5 to 8 when compared to vulcanized samples.

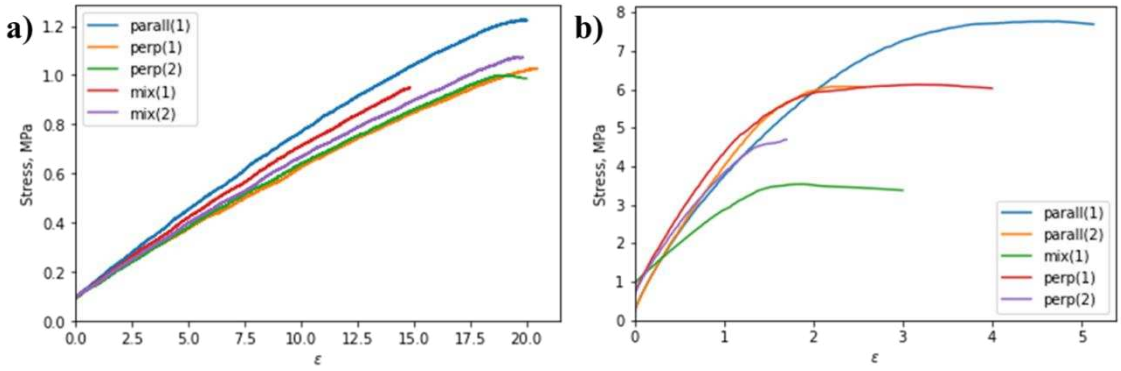

Figure 7. Engineering stress-strain curves obtained for large samples in tension: a) vulcanized samples before carbonization, b) carbonized samples.

Table 1. The mechanical properties of large samples obtained using Zwick/Roell Z02 universal testing machine.

Composition	E, MPa	σ_{max}, MPa	Elongation till rupture, %
Vulcanized samples before carbonization			
parall(1)	10.0	1.2	23
perp(1)	5.7	1.0	22
perp(2)	6.6	1.0	21
mix(1)	6.7	1.0	15
mix(2)	6.1	1.1	21

 doi:10.20944/preprints202310.0222.v1

Carbonized samples			
parall(1)	282	7.8	5
parall(2)	334	6.1	3
mix(1)	203	3.5	5
perp(1)	396	6.1	6
perp(2)	281	4.7	2

It is worth noting that the carbonization process causes significant embrittlement of the composite. In particular, when the reinforcing hairs are oriented parallel to the tension axis, there is a decrease in elongation to rupture of more than 4 times. Similarly, for samples with the hair orientation perpendicular to the tension axis the drop is more than 7 times. Finally, for samples with the mixed hair orientation distribution the reduction of elongation to rupture for about 3 times was observed. The reduction in deformability (elongation to rupture) of the carbonized composites compared to the vulcanized samples is primarily attributed to the formation of a structure with high carbon content (C-C) incorporating a small proportion of chemical bonds such as C-H, N-H, and C-OH, as well as an increase in volume porosity.

The stress-strain curves obtained for miniature samples are shown in Figures 8 and 9. The correspondent mechanical characteristics were estimated and summarized in Table 2.

The analysis of miniature samples provides more robust results from statistical point of view due to the higher number of specimens. In this case, hair reinforcement results in a more than tenfold increase from 3.7-3.8 to 40 MPa in Young's modulus for the composite materials in the vulcanized state compared to raw elastomeric materials.

The unfilled composite exhibits an increase of over 7 times in the elastic modulus due to the carbonization. On the other hand, reinforced composites show somewhat lower increase - 2.5 times for unnotched specimens and a modest rise of no more than 20 % for notched specimens. The growth in Young's modulus caused by matrix carbonization as we believe is weakened by the factors of porosity that forms due to the thermal degradation of both rubber matrix and reinforcing hair biopolymer. Additionally, the introduction of a notch moderately decreases the effective elastic modulus in the unfilled composite and significantly reduces it by almost 2 times in the reinforced composite. The changes of tensile strength in the studied composite materials are similar to the variations in elastic modulus. The reinforcement of elastomer matrix with human hairs gives raise of tensile strength of about 3 times for both notched and unnotched vulcanized samples. The notches themselves, however, reduce the effective strength, as commonly expected. Carbonization of vulcanized composites results in a more significant strength increase - by a factor of 18 - for unreinforced specimens than reinforced ones, similarly to elastic modulus.

Preprints (www.preprints.org) | NOT PEER-REVIEWED | Posted: 4 October 2023 doi:10.20944/preprints202310.0222.v1

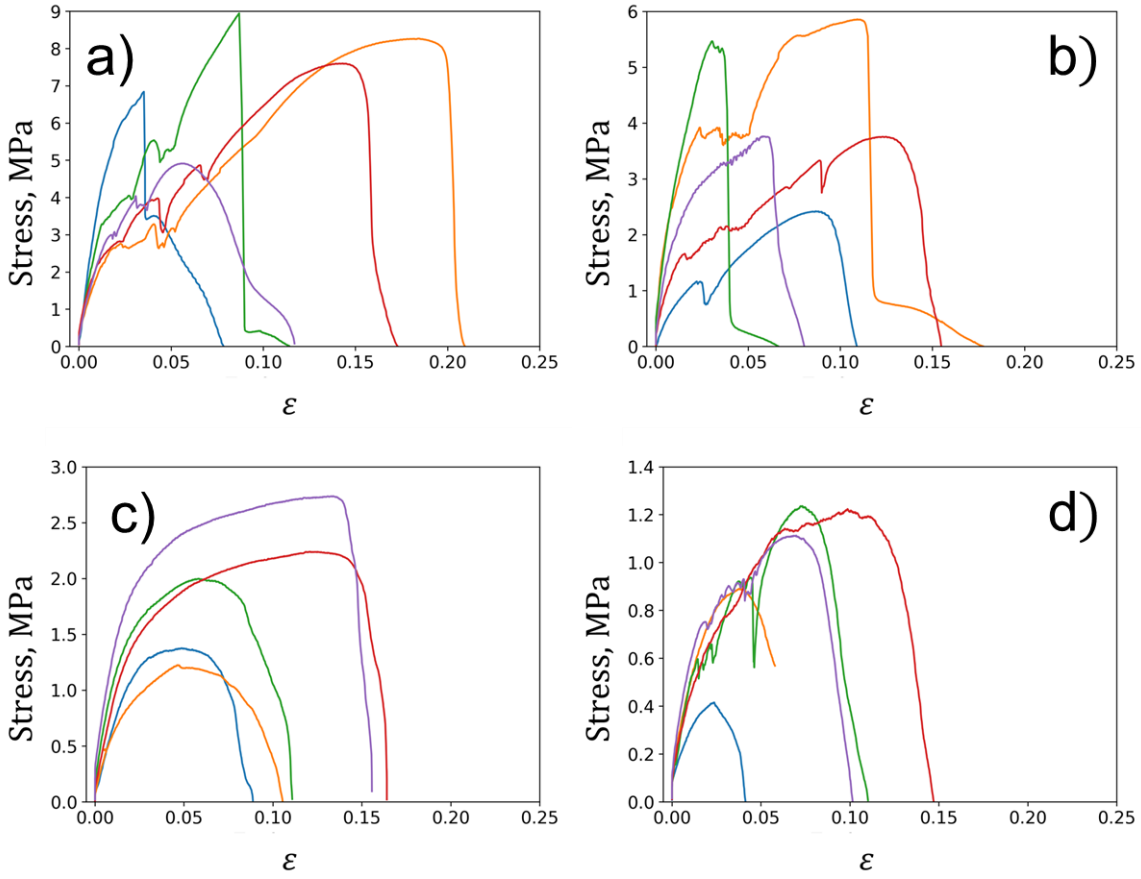

Figure 8. The stress-strain curves obtained for vulcanized miniature samples under tension: a) without fillers, b) without fillers with notches, c) with hair reinforcement, d) with hair reinforcement and notches.

To sum up, hair reinforcement and notching in vulcanized composites reduce the overall deformability (elongation to rupture), while carbonization tends to improve it by 60 % in reinforced samples. It is assumed that the cohesive porosity effectively eliminates cracks at the pores or redirects them away from the shortest propagation paths. Furthermore, the reinforcement significantly enhances the durability of composites effectively blocking cracks and deviating them from the straight path.

The total work to failure of composites exhibits several distinctive features:

a) obvious decrease in this value in notched compared to unnotched specimens (2 and more times);

b) increase of the work of fracture resulting from carbonization (3-4 times);

c) unfavorable impact of reinforcement on the work of fracture (presumably caused by decrease in deformability and effective cross-section).

Preprints (www.preprints.org) | NOT PEER-REVIEWED | Posted: 4 October 2023 doi:10.20944/preprints202310.0222.v1

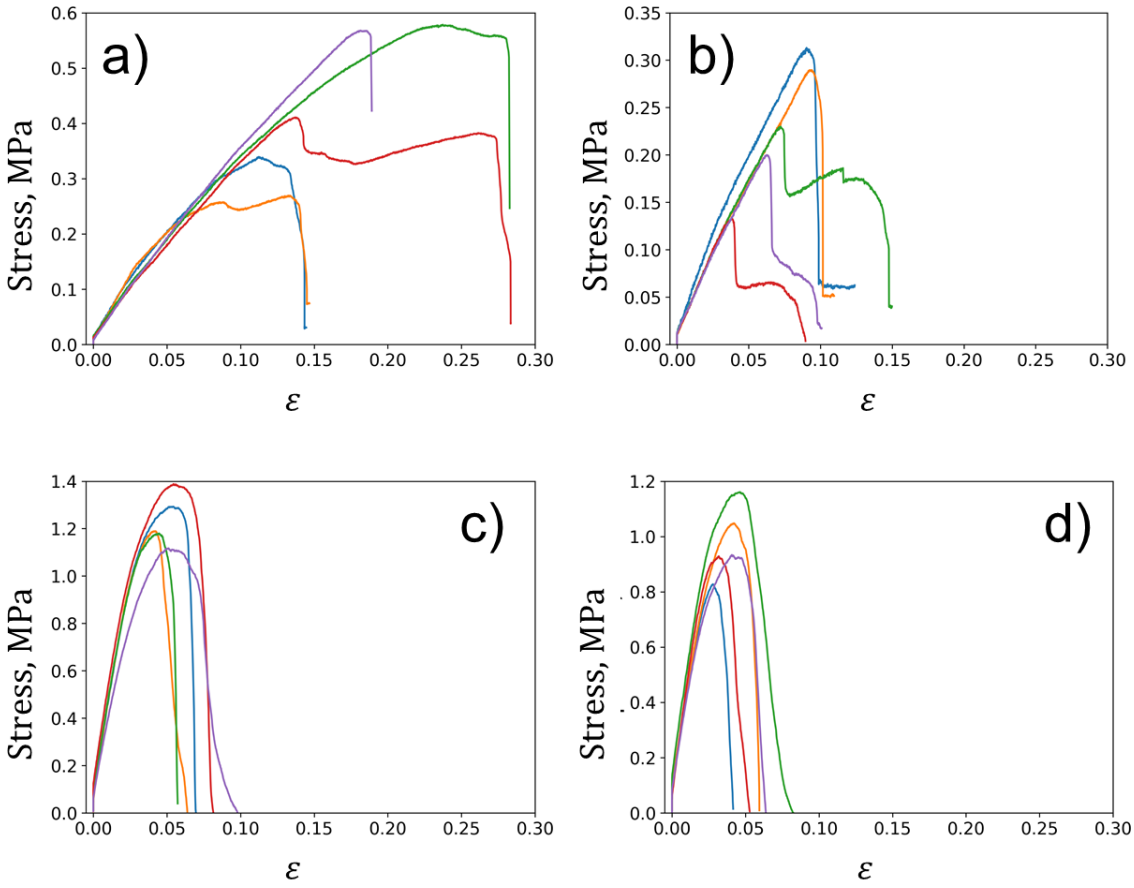

Figure 9. The stress-strain curves obtained for carbonized miniature samples in tension mode: a) without fillers, b) without fillers with notches, c) with hairs reinforcement, d) with hairs reinforcement and notches.

Table 2. The mechanical properties of miniature samples obtained using Deben Microtest 1 kN universal testing machine.

	With notches	With hairs	Young's modulus, MPa	Tensile strength, MPa	Elongation till rupture, %	Fracture work, N·mm
Vulcanized			3.7±0.1	0.4±0.1	21±3	10±2
	+		3.8±0.2	0.23±0.03	11±1	2.2±0.4
		+	42±2	1.23±0.04	7±1	6±1
	+	+	39±1	1.0±0.1	6±1	4±1
Carbonized			298±27	7.3±0.6	14±2	81±21
	+		257±54	4.3±0.6	12±2	39±10
		+	103±16	1.9±0.2	12±1	19±5
	+	+	53±6	1.0±0.1	9±2	7±2

3.3. Microstructure characterization by photoacoustic microscopy

Photoacoustic images of human hairs and raw elastomer matrix are shown in Figure 10. The colors in the images correspond to the acoustic signals acquired at a frequency range of 11-99 MHz. The photoacoustic signal of the unfilled and reinforced rubber composite taken at different projections is depicted in Figure 11. The findings demonstrate that the reliable identification of reinforcing hairs can be achieved with this technique, providing good spatial resolution up to several microns. This confirms the random orientation and uniform distribution of hair throughout the

Preprints (www.preprints.org) | NOT PEER-REVIEWED | Posted: 4 October 2023 doi:10.20944/preprints202310.0222.v1

matrix. Rubber matrix, as it is, generates diffuse background signal, perhaps, due to surface refraction effects. When a laser beam is incident at the rubber-air interface, some of the light is reflected, some is absorbed, and some is transmitted into the rubber material. The absorbed light generates a photoacoustic signal due to the thermal expansion of the material and subsequent generation of ultrasound waves. In the case of rubber matrices, photons undergo multiple scattering events as they propagate through the material. These scattering events cause light to deviate from its original path and result in the diffusion of light within the rubber matrix. As a consequence, the generated photoacoustic signals also exhibit a diffuse nature since the absorbed light is distributed throughout the volume of the matrix rather than being confined to specific absorption locations. However, the photoacoustic microscopy fails to produce adequate acoustic signals to distinguish and recognize reinforcing hair within carbonized samples. It is probable that the thermal destruction of hair biopolymers leads to the removal of photoactive melanin in the hairs.

These findings support the ability of non-invasive visualization of reinforcing hair within composite materials. This method can subsequently facilitate the 3D reconstruction of the material structure and the corresponding finite element analysis of the deformation behavior. Moreover, it offers the potential to transition to photoacoustic 3D tomography for composites and enable non-destructive quality control of such materials. The use of markers in a polymer matrix provides opportunities for a variety of *operando* tests.

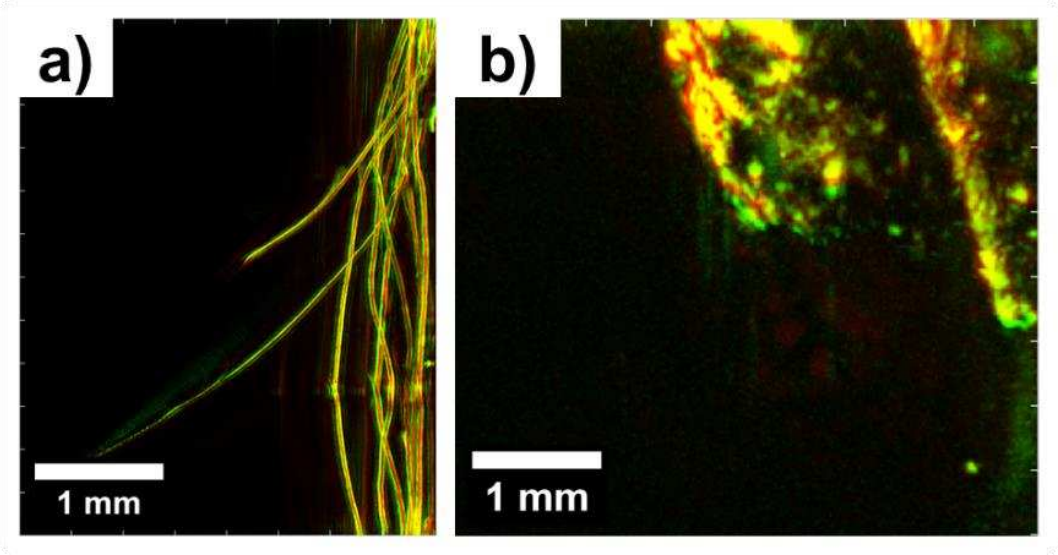

Figure 10. The photoacoustic signal obtained for a) human hairs in XZ plane and b) unfilled elastomer material in XY plane at the frequency range from 11 to 99 MHz.

Preprints (www.preprints.org) | NOT PEER-REVIEWED | Posted: 4 October 2023 doi:10.20944/preprints202310.0222.v1

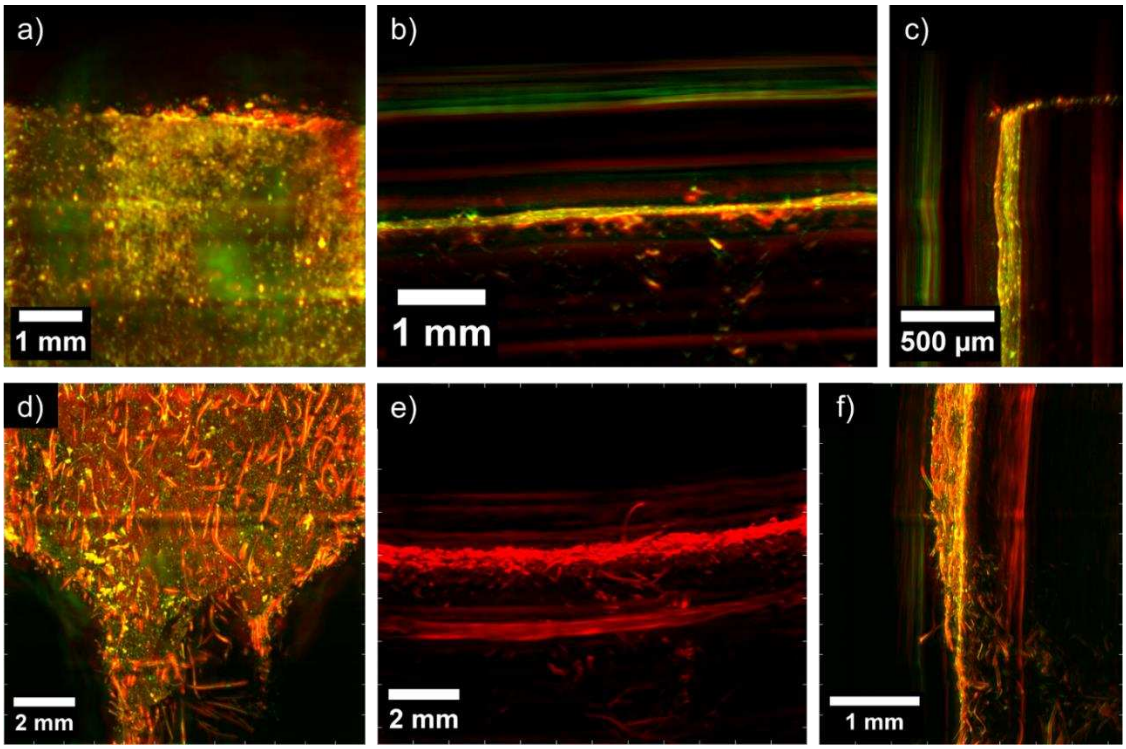

Figure 11. The photoacoustic signal obtained for: a,b,c) unfilled, and d,e,f) reinforced vulcanized composite at the frequency range from 11 to 99 MHz (a-d, f) and 11-33 MHz (e). a, d) XY plane; b, e) YZ plane; c, f) XZ plane.

4. Conclusions

Composite and hybrid materials with biopolymer matrices or fillers are crucial for promoting sustainable development through the use of renewable resources as raw materials. The significance of these materials cannot be overstated. Creating such materials encounters common difficulties seen in composite materials. such as the requirement for optimal spatial arrangement of reinforcing structural elements, improved adhesion between filler and matrix, and quality control of finished products via non-destructive methods.

This study is focused on analyzing the structure and physical as well as mechanical properties of composite materials. The materials were made of vulcanized and carbonized butadiene-nitrile rubber and were strengthened with biopolymer fibers (human hairs). The experimental methods used included photoacoustic imaging of hair inside the matrix using nanostructured melanin as a marker. From the study, the following inferences can be made:

- The feasibility of the proposed technique for producing composite materials that exhibit a marked increase in physical and mechanical properties (specifically elastic modulus and tensile strength), while maintaining acceptable levels of deformability and fracture work, has been verified in comparison to unreinforced rubber.
- The experimental results confirm a significant enhancement in properties for both vulcanized and carbonized NR matrix rubber under varying hair orientations (i.e. parallel, perpendicular, and mixed) relative to the tensile axis with and without notches (i.e. stress concentrators).
- Notably, the hair-reinforced composites display a unique fracture behavior that leads to high specimen survivability even after the onset of fracture.
- The study utilizes high-resolution scanning electron microscopy to analyze the fracture surface and proposes mechanisms for fracture development. Specifically, it identifies the structural characteristics of the matrix and reinforcing fibers that effectively block brittle crack propagation.

- The effectiveness of using nanostructured melanin as a marker for photoacoustic imaging of fibers within the matrix is also demonstrated. High-resolution images were acquired to observe the reinforcing fibers within the elastomeric matrix.

Acknowledgments: This work was supported by the Federal Academic Leadership program "Priority 2030" under the "Increase Competitiveness" program of the National University of Science and Technology MISIS (grant number K1-2022-032).

References

1. Sezgin, H.; Yalcin Enis, I. Human Hair Fiber as a Reinforcement Material in Composite Structures. 2nd International Symposium on Innovative Approaches n Scientific Studies, Samsun, Turkey, 2018, 3, 880-883.
2. Espín-Lagos, S. M.; Arias, A. R. R.; Guamanquispe-Toasa, J. P.; Avila, E. M. B. Long and Short Human Hair Fiber-Reinforced Polymer Composites: Mechanical Properties for Engineering Applications. MSF 2022. https://doi.org/10.4028/p-p2mjlo
3. Brandt, A. M. Fibre reinforced cement-based (FRC) composites after over 40 years of development in building and civil engineering. Compos. Struct. 2008, 86 (1–3), 3-9. DOI: 10.1016/j.compstruct.2008.03.006
4. Naik, H.; Naikoo, N. A.; Dar, S. A.; Showket, M.; Muhamm, S. A. Use of horse hair as fiber reinforcement in concrete Int. J. Adv. Res. 2015, 3, 1569-1572. ISSN: 2320-5407
5. Verma, A.; Singh, V. K. Mechanical, microstructural and thermal characterization of epoxy-based human hair-reinforced composites (2019). J. Test. Eval. 2019, 47 (2), 1193-1215. DOI: 10.1520/JTE20170063
6. Rojas-Martínez, L. E.; Flores-Hernandez, C. G.; López-Marín, L. M.; Martinez-Hernandez, A. L.; Thorat, S. B.; Reyes Vasquez, C. D.; Del Rio-Castillo, A. E.; Velasco-Santos, C. 3D printing of PLA composites scaffolds reinforced with keratin and chitosan: Effect of geometry and structure. Eur. Polym. J. 2020, 141, 110088. DOI: 10.1016/j.eurpolymj.2020.110088
7. Müllner, A. R. M.; Pahl, R.; Brandhuber, D.; Peterlik, H. Porosity at Different Structural Levels in Human and Yak Belly Hair and Its Effect on Hair Dyeing. Molecules 2020, 25 (9), 2143. DOI: 10.3390/molecules25092143
8. Stanić, V.; Bettini, J.; Montoro, F.; et al. Local structure of human hair spatially resolved by sub-micron X-ray beam. Sci. Rep. 2015, 5, 17347. DOI: 10.1038/srep17347
9. Ignatyev, S. D.; Statnik, E. S.; Ozherelkov, D. Y.; Zherebtsov, D. D.; Salimon, A. I.; Chukov, D. I.; Tcherdyntsev, V. V.; Stepashkin, A. A.; Korsunsky, A. M. Fracture Toughness of Moldable Low-Temperature Carbonized Elastomer-Based Composites Filled with Shungite and Short Carbon Fibers. Polymers 2022, 14 (9), 1793. DOI: 10.3390/polym14091793
10. Statnik, E. S.; Ignatyev, S. D.; Stepashkin, A. A.; Salimon, A. I.; Chukov, D.; Kaloshkin, S. D.; Korsunsky, A. M. The Analysis of Micro-Scale Deformation and Fracture of Carbonized Elastomer-Based Composites by In Situ SEM. Molecules 2021, 26 (3), 587. DOI: 10.3390/molecules26030587
11. Stepashkin, A. A.; Chukov, D. I.; Kaloshkin, S. D.; Pyatov, I. S.; Deniev, M. Y. Carbonised composite materials based on elastomers filled with carbon nanofillers. Micro Nano Lett. 2018, 13 (5), 588-590. DOI: 10.1049/mnl.2017.0235
12. Cvjetinovic, J.; Salimon, A. I.; Novoselova, M. V.; Sapozhnikov, P. V.; Shirshin, E. A.; Yashchenok, A. M.; Gorin, D. A. Photoacoustic and Fluorescence Lifetime Imaging of Diatoms. Photoacoustics 2020, 100171. DOI: 10.1016/j.pacs.2020.100171
13. Chetyrkina, M. R.; Cvjetinovic, J.; Fedorov, F. S.; Perevoschikov, S. V.; Prikhozhdenko, E. S.; Mikladal, B. F.; Gladush, Y. G.; Nasibulin, A. G.; Gorin, D. A. Carbon Nanotube Microscale Fiber Grid as an Advanced Calibration System for Multispectral Optoacoustic Imaging. ACS Photonics 2022, 9 (10), 3429-3439. DOI: 10.1021/acsphotonics.2c01074